RECONSTRUCTING SMALL SURFACE PATCHES FROM MULTIPLE IMAGES

Toni Schenk
Charles K. Toth

Department of Geodetic Science and Surveying
The Ohio State University, Columbus, Ohio 43210-1247
USA

Commission III

ABSTRACT

Matching multiple images simultaneously greatly increases the reliability of determining conjugate points automatically. It offers significant advantages for aerotriangulation because tie points cannot only be determined automatically but also more reliably. In this paper we develop models where the matching is combined with reconstructing a surface patch geometrically and radiometrically from multiple image patches.

KEY WORDS: Image Matching, Aerotriangulation, Machine Vision.

1. INTRODUCTION

Determining conjugate points is a fundamental task that occurs in almost any photogrammetric application. In digital photogrammetry it has become customary to call this process *image matching*. It is fascinating to observe the development of image matching during the last decade. Much progress has been made since Ackermann (1984) and Förstner (1984) presented the first rigorous mathematical models for the image matching process. Apart from extending the basic mathematical model by introducing geometrical constraints (see, e.g., Grün & Baltsavias, 1988), a decisive step was to combine matching with reconstructing the surface (see e.g. Wrobel, 1987; Helava, 1987; Ebner *et al.*, 1987).

Ebner and Heipke (1988) propose a new approach where matching several images and surface reconstruction is treated as a simultaneous adjustment problem. Matching multiple image patches is of great practical importance, most notably in aerotriangulation where as many as nine photographs may partially overlap. Identifying and measuring tie points, particularly between strips, is a notorious problem, since only two photographs can be viewed stereoscopically at the same time. The reliability and accuracy of tie points is expected to significantly increase when multiple image matching methods are employed.

The purpose of this paper is to formulate suitable mathematical models for rigorously solving the multiple image matching problem. We describe a general solution by introducing a geometric and radiometric relation between a surface patch and the corresponding image patches. We then investigate several geometric transformation models between object and image space, including linearized observation equations. We conclude with describing two approaches of using multiple image matching in aerotriangulation. The first approach is the most general one where the exterior orientation, the surface patches with elevations (DEM) and gray levels are all determined simultaneously. In the second approach conjugate points are determined independently from one another and without the exterior orientation parameters. This solution corresponds to the traditional method where all points are individually measured and then entered into a block adjustment.

2. GENERAL APPROACH

Fig. 1 depicts four images $I_1, \ldots, I_4$ with image patches $p_1, \ldots, p_4$ covering the surface patch S. To generalize let p be the number of image patches, size $n \times n$ pixels. Associated with every image patch p_i is a gray level function $g_i(x, y)$. We may consider the gray levels as observed.

The surface patch S is represented as a DEM with a resolution of $m \times m$ grid points, $m \ll n$. The task is now to reconstruct the surface patch S from the observed gray levels of the image patches. This involves both, geometric and radiometric reconstruction. Let $Z(X, Y)$ be the geometric function and $G(X, Y)$ the radiometric function for representing the surface patch S. Capital letters are used to better differentiate object space functions and variables from their counterparts in image space. Obviously, the image functions $g_i(x, y)$ correspond to $G(X, Y)$, the gray level distribution of the surface patch S. The discrete representation of $Z(X, Y)$ can be considered the DEM of S. The reconstruction of S involves $2m^2$ parameters (m^2 elevations, m^2 gray levels).

Since S is small we may approximate it by a Lambertian surface. The gray levels of the image patches are then directly related to the gray levels of the surface patch. Suppose the surface is flat and parallel to all image patches. In this (unrealistic) case, the gray levels of S would simply be the mean of the gray levels of all image patches.

Next, we need to define the geometrical relationship between the image patches and the surface patch. This is accomplished by a geometrical transformation $\mathbf{T^g}$. Combining the geometric and radiometric relationship leads to the following non linear observation equations:

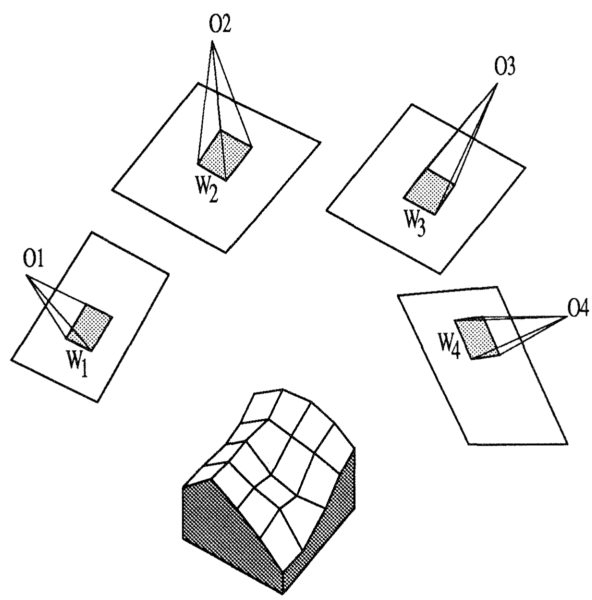

Figure 1: Multiple image patches covering the same surface patch S

$$\mathbf{r_i} = G(X,Y) - \mathbf{T_i^r}\left[g_i\left(\mathbf{T_i^g}(x,y)\right)\right] \quad (1)$$

with $\mathbf{r_i}$, $i = 1,2,\ldots,p$ the residual vectors, dimension m^2, and $G(X,Y)$ the gray level function of the surface patch S. Each image patch contributes m^2 equations leading to a total of pm^2 observation equations. The parameters to be determined include the gray levels $G(X,Y)$ and the elevations $Z(X,Y)$ of the surface patch, as well as the transformation parameters $\mathbf{T_i^r}$ and $\mathbf{T_i^g}$ for every image patch.

With equation 1 the task of reconstructing S from multiple image patches is formulated as a least squares problem where the gray level differences between the image patches and the surface are minimized by varying the surface shape $Z(X,Y)$, the surface gray levels $G(X,Y)$ and the exterior orientation of the image patches. This takes the concept of matching in object space a step further to include the determination of the gray levels of the surface. Since the image patches p_i have to be resampled with the geometric transformation $\mathbf{T^g}$ (which in turn is a function of the unknown exterior orientation parameters!) the image patches must be larger $(n \times n)$ than the surface patch $(m \times m)$, hence $m \ll n$.

2.1. Geometric Transformation T^g

There are several possibilities to model the geometric transformation between the image patches p_i and the surface $Z(X,Y)$.

1. The collinearity equations are the most general transformation between surface and images. The transformation parameters comprise the exterior orientation elements of the images I_i.
2. Since the image patches are rather small the central projection may be approximated by a parallel projection. In that case the transformation parameters would include the spatial direction of the projection (3 angles), a translation of the image patch and a scale factor.
3. It is also conceivable to approximate the surface by an analytical function and determine its parameters.
4. As a further simplification of model 3 we approximate the surface S by a plane. The relationship between an image patch and S can now be expressed by a projective transformation which in turn may be approximated by an affine transformation. This would correspond to the classical case of least squares matching with shape parameters.

2.2. Radiometric Transformation T^r

Based on the assumption that S is a Lambertian surface a linear radiometric relationship of the form

$$\mathbf{T^r} = r_0 + r_1\left(g_i(x,y)\right) \quad (2)$$

exists between the image patches. It may even be adviseable to perform the radiometric adjustment prior to the matching. Therefore, we exclude the radiometric transformation from the following considerations.

3. GEOMETRIC TRANSFORMATION MODELS

3.1. Central Projection

We linearize the observation equation 1 under the assumption that $\mathbf{T^g}$ is a central projection. Disregarding the radiometric transformation and dropping the indices i for denoting i^{th} image patch equation 1 reads

$$\mathbf{r} = G(X,Y) - g\left(T_x, T_y\right) \quad (3)$$

where $g(T_x, T_y)$ needs to be linearized with respect to the exterior orientation parameters and Z.

$$\begin{aligned}\mathbf{r} &= G(X,Y) - g^0(T_x^0, T_y^0) - \sum_{i=1}^{7}\left(\frac{\vartheta g\left(T_x,T_y\right)}{\vartheta T_x}\frac{\vartheta T_x}{\vartheta a_i} + \right. \\ &+ \left.\frac{\vartheta g\left(T_x,T_y\right)}{\vartheta T_y}\frac{\vartheta T_y}{\vartheta a_i}\right)\Delta a_i\end{aligned} \quad (4)$$

with

$$\begin{aligned} g_x &= \frac{\vartheta g\left(x,y\right)}{\vartheta T_x} \\ g_y &= \frac{\vartheta g\left(x,y\right)}{\vartheta T_y}\end{aligned} \quad (5)$$

we obtain

$$\mathbf{r} = G(X,Y) - g^0(T_x^0, T_y^0) - \sum_{i=1}^{7}\left(g_x\frac{\vartheta T_x}{\vartheta a_i} + g_y\frac{\vartheta T_y}{\vartheta a_i}\right)\Delta a_i \quad (6)$$

where g_x, g_y are the gradients in $x-$ and $y-$ directions, a_i the partial derivatives of the collinearity equations. The initial gray levels $g^0(T_x^0, T_y^0)$ of the image patch are determined by transforming the initial elevations $Z^0(X,Y)$ to the image with the initial collinearity equations T_x^0, T_y^0. The parameters Δa_i include the 6 exterior orientation elements and ΔZ, the unknown elevations of the surface patch. Finally, $G(X,Y)$ are the unknown gray levels of the surface.

3.2 Parallel Projection

If the exterior orientation in the collinearity model is determined from one image patch only the normal equation system will be ill-conditioned. The perspective center is only weakly determined by the small image patch since the intersecting bundle rays form very acute angles. Of course, if the same image is involved in several well distributed surface patches, the situation improves, but only if a simultaneous adjustment is performed.

If the surface patches are determined individually then a parallel projection should be used instead of the central projection. The direction of the projection is defined by the bundle ray through the center of the surface patch (see Fig. 2). This direction can easily be determined in image space. Let $[x_s, y_s, -c]^T$ be the center of the image patch in the traditional photocoordinate system (origin at perspective center). The bundle ray through the center of the patch is then defined by the following equations:

$$\begin{aligned} z &= nx & y &= mx \\ n &= \frac{c}{x_c} & m &= \frac{y_c}{x_c} \end{aligned} \tag{7}$$

The angles α, β, γ determine the spatial direction of the bundle ray that represents the image patch.

$$\begin{aligned} cos(\alpha) &= \frac{1}{\sqrt{1+m^2+n^2}} \\ cos(\beta) &= \frac{m}{\sqrt{1+m^2+n^2}} \\ cos(\gamma) &= \frac{n}{\sqrt{1+m^2+n^2}} \end{aligned} \tag{8}$$

With these three independent angles about the axis of the photo coordinate system the rotation matrix $\mathbf{R}$ is formed in the usual fashion. The corresponding rotation matrix $\mathbf{R_s}$ in the object space coordinate system is obtained by multiplying $\mathbf{R}$ with the rotation matrix from the exterior orientation $\mathbf{R_e}$

$$\mathbf{R_s} = \mathbf{R_e}\mathbf{R} \tag{9}$$

If we rotate the surface patch S by $\mathbf{R_s}$ then the projection becomes parallel to z in the photo coordinate system. Since we deal with a parallel projection the object/image space relationship is trivial, that is, $x = X', y = Y'$ where x, y are the photo coordinates and X', Y' the rotated surface coordinates.

Now we complete the geometric transformation by adding a translation vector $[x_t, y_t]^T$ and a scale factor s. This compensates for not including the perspective center in the transformation. Finally, the following transformation equations describe the parallel projection

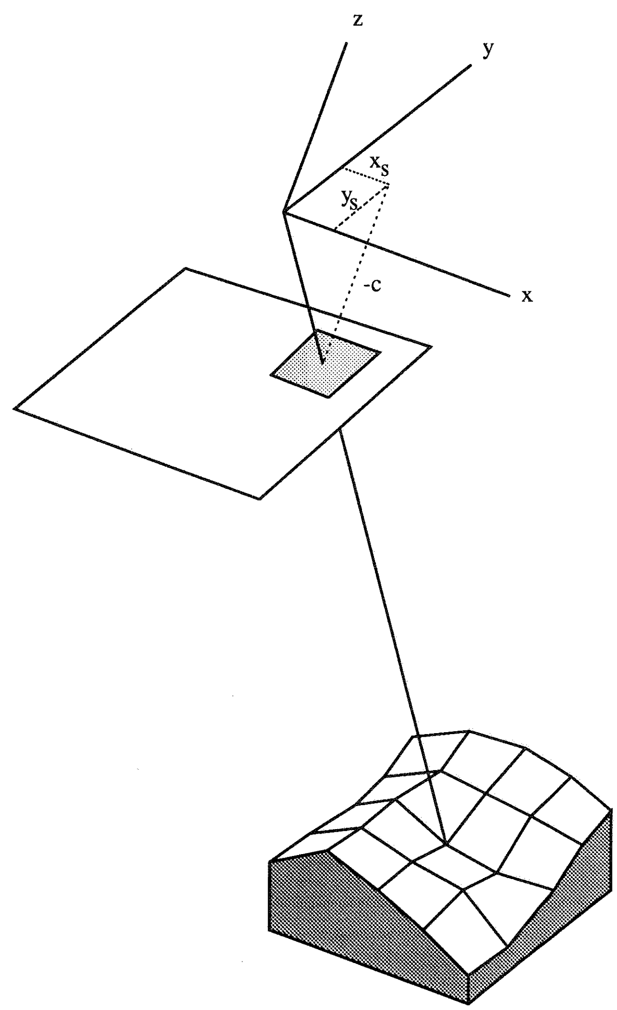

Figure 2: Direction of parallel projection defined by bundle ray through center of surface patch S

$$\begin{aligned} x &= (r_{11}X + r_{12}Y + r_{13}Z)\,s + x_t \\ y &= (r_{21}X + r_{22}Y + r_{23}Z)\,s + y_t \end{aligned} \tag{10}$$

Linearizing the general observation equations 3 with respect to the geometric transformation of equation 10 we obtain equation 11 which corresponds to equation 6

$$\mathbf{r} = G(X,Y) - g^0(T_x^0, T_y^0) - \sum_{i=1}^{7}\left(g_x \frac{\vartheta T_x}{\vartheta a_i} + g_y \frac{\vartheta T_y}{\vartheta a_i}\right)\Delta a_i \tag{11}$$

with the partial derivatives

$$\begin{aligned} \frac{\vartheta T_x}{\vartheta \alpha} &= a_1^x = s\,[0,0,0]\begin{bmatrix} X \\ Y \\ Z \end{bmatrix} \\ \frac{\vartheta T_y}{\vartheta \alpha} &= a_1^y = s\,[r_{31}, r_{32}, r_{33}]\begin{bmatrix} X \\ Y \\ Z \end{bmatrix} \\ \frac{\vartheta T_x}{\vartheta \beta} &= a_2^x = -s\cos(\gamma)\,[r_{31}, r_{32}, r_{33}]\begin{bmatrix} X \\ Y \\ Z \end{bmatrix} \end{aligned}$$

$$\frac{\vartheta T_y}{\vartheta \beta} = a_2^y = s\sin(\gamma)\,[r_{31}, r_{32}, r_{33}] \begin{bmatrix} X \\ Y \\ Z \end{bmatrix}$$

$$\frac{\vartheta T_x}{\vartheta \gamma} = a_3^x = s\,[r_{21}, r_{22}, r_{23}] \begin{bmatrix} X \\ Y \\ Z \end{bmatrix} \quad (12)$$

$$\frac{\vartheta T_y}{\vartheta \gamma} = a_3^y = s\,[-r_{11}, -r_{12}, -r_{13}] \begin{bmatrix} X \\ Y \\ Z \end{bmatrix}$$

$$\frac{\vartheta T_x}{\vartheta s} = a_4^x = s\,[r_{11}, r_{12}, r_{13}] \begin{bmatrix} X \\ Y \\ Z \end{bmatrix}$$

$$\frac{\vartheta T_y}{\vartheta s} = a_4^y = [r_{21}, r_{22}, r_{23}] \begin{bmatrix} X \\ Y \\ Z \end{bmatrix}$$

$$\frac{\vartheta T_x}{\vartheta x_t} = a_5 = 1$$

$$\frac{\vartheta T_y}{\vartheta y_t} = a_6 = 1$$

$$\frac{\vartheta T_x}{\vartheta Z} = s r_{13}$$

$$\frac{\vartheta T_y}{\vartheta Z} = s r_{23}$$

where r_{ij} are the elements of the rotation matrix $\mathbf{R_s}$ in equation 9.

4. APPLICATIONS

There are several practical applications for multiple image matching. We focus on aerotriangulation and describe briefly the simultaneous adjustment of surface patches within a block. Aerotriangulation consists of several tasks, for example point preparation, point transfer, measuring, adjustment, and analysis. Oviously, multiple image matching is related to transferring and measuring points. However, we may combine the matching process for individual points with the blockadjustment. For the following discussion we assume that good approximations for all tie points are available. How to determine good approximations automatically is a problem in its own right and is not treated here.

4.1. Automatic Aerotriangulation

The model derived in 3.1. is suitable for an automatic aerotriangulation. The parameters in the observation equations (6) comprise the exterior orientation elements of the images whose patches are involved in the reconstruction of the surface patch S, and the elevations and gray levels of S. Assuming a surface patch size of $m \times m$ grid cells that corresponds approximately to the pixel size of the images we obtain a total pm^2 observation equations for p image patches. Suppose we now move to the next surface patch and repeat the same procedure. Some of the images involved in the previous patch participate also in the new patch. We note that the images involved in both patches relate the new set of observation equations with the previous one. Obviously, adding more and more surface patches which partially share the same images is analogous to measuring points on photographs forming a block.

Suppose we have a block of three strips with four photographs per strip and regularly distributed surface patches such that on every image at least nine surface patches are visible. This would lead to approximately 40 surface patches. We further assume that the size of every surface patch is 13×13. The number of unknowns to be determined is 12×6 exterior orientation elements plus $40 \times 13 \times 13$ elevations and $40 \times 13 \times 13$ gray values for the 40 surface patches. Thus, the total number of unknowns is 13592 and the number of observation equations is $4 \times 40 \times 13 \times 13 = 27040$, assuming that a surface patch shows on four photographs.

As shown in Agouris and Schenk (1992) the structure of the normal equation matrix is such that the unknown gray values can easily be eliminated. Thus, the size of the reduced normal equations would be 6832 in our example. This is still a large system considering the small block. A reasonable alternative then is to determine the surface patches independently and to introduce them later in the aerotriangulation. In this case, the model described in 3.2. should be used.

5. REFERENCES

Ackermann, F. 1984. High Precision Digital Image Correlation. *Institute of Photogrammetry*, TU Stuttgart, Vol. 9, p. 231-243.

Agouris, P., T. Schenk 1992. Multiple Image Matching. *International Archives of Photogrammetry & Remote Sensing*, ISPRS XVII Congress, Washington, D.C..

Ebner, H., Ch. Heipke, 1988. Integration of Digital Image Matching and Object Surface Reconstruction. *International Archives of Photogrammetry & Remote Sensing*, ISPRS XVI Congress, Vol. 27, Part B 11, pp III-534 - III-545.

Förstner, W., 1984. Quality Assessment of Object Location and Point Transfer Using Digital Image Correlation Techniques. *International Archives of Photogrammetry & Remote Sensing*, ISPRS XV Congress, Vol. 25, Part A3a, pp 197-219.

Grün, A., E. Baltsavias, 1988. Geometrically Constrained Multiphoto Matching. *Photogrammetric Engineering & Remote Sensing*, Vol. 54, No. 5, pp. 633-641.

Helava, U., 1988. Object-Space Least-Squares Correlation. *Photogrammetric Engineering & Remote Sensing*, Vol. 54, No. 6, pp. 711-714.

Wrobel, B., 1988. Facets Stereo Vision (Fast Vision) - A new Approach to Computer Stereo Vision and to Digital Photogrammetry. *Proc. Intercomm. Conference of ISPRS on Fast Processing of Photogr. Data*, Interlaken, pp. 231-258.